analytical chemistry

Article

pubs.acs.org/ac

Proteomic Analysis of Nuclei Dissected from Fixed Rat Brain Tissue Using Expression Microdissection

A. R. Blackler,[†] N. Y. Morgan,[‡] B. Gao,[§] L. R. Olano,[∥] M. D. Armani,[†] E. Romantseva,[‡] J. W. Kakareka,[⊥] R. F. Bonner,[⊗] S. Mukherjee,[†] B. Xiao,[⊥] K. Tran,[⊗] T. J. Pohida,[⊥] M. R. Emmert-Buck,*[,†] M. A. Tangrea,[†] and S. P. Markey[§]

[†]National Cancer Institute, NIH, Bethesda, Maryland 20892, United States

[‡]National Institute of Biomedical Imaging and Biomedical Engineering, NIH, Bethesda, Maryland 20892, United States

[§]National Institute of Mental Health, NIH, Bethesda, Maryland 20892, United States

[∥]RTB, National Institute of Allergy and Infectious Disease, NIH, Bethesda, Maryland 20892, United States

[⊥]Center for Information Technology, NIH, Bethesda, Maryland 20892, United States

[⊗]National Institute of Child Health and Human Development, NIH, Bethesda, Maryland 20892, United States

Supporting Information

ABSTRACT: Expression microdissection (xMD) is a high-throughput, operator-independent technology that enables the procurement of specific cell populations from tissue specimens. In this method, histological sections are first stained for cellular markers via either chemical or immuno-guided methods, placed in close contact with an ethylene vinyl acetate (EVA) film, and exposed to a light source. The focal, transient heating of the stained cells or subcellular structures melts the EVA film selectively to the targets for procurement. In this report, we introduce a custom-designed flashcube system that permits consistent and reproducible microdissection of nuclei across an FFPE rat brain tissue section in milliseconds. In addition, we present a method to efficiently recover and combine captured proteins from multiple xMD films. Both light and scanning electron microscopy demonstrated captured nuclear structures. Shotgun proteomic analysis of the samples showed a significant enrichment in nuclear localized proteins, with an average 25% of recovered proteins localized to the nucleus, versus 15% for whole tissue controls ($p < 0.001$). Targeted mass spectrometry using multiple reaction monitoring (MRM) showed more impressive data, with a 3-fold enrichment in histones, and a concurrent depletion of proteins localized to the cytoplasm, cytoskeleton, and mitochondria. These data demonstrate that the flashcube-xMD technology is applicable to the proteomic study of a broad range of targets in molecular pathology.

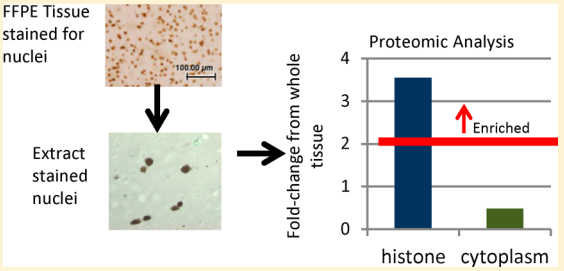

Laser capture microdissection (LCM) was developed in the mid-1990s as a means to acquire specific cells from a heterogeneous tissue specimen.[1] The isolation of distinct cell populations, combined with newer high-throughput genomic profiling technologies, now allows investigators to perform sensitive downstream biomolecular analyses.[2]

LCM has been combined more recently with proteomic analyses, permitting identification of potential disease related biomarkers in tissue.[3,4] LCM and proteomic techniques have identified protein expression changes in breast cancer,[5,6] new metastatic tumor markers for colorectal cancer,[7] and have been used to profile the proteome of mouse brain microvascular endothelium.[8]

However, proteomic evaluation of LCM-acquired tissue can be difficult due to inherent limitations of the technology. First, laser dissection is generally laborious, requiring hours of operator and instrument time to collect the microgram quantities of protein required for comprehensive proteomic analysis. Additionally, while LCM allows for microdissection of single cells, the resolution (~10 μm) is limiting and subcellular organelles cannot be easily isolated.[9]

Expression microdissection (xMD) is a conceptually different approach that enables retrieval of specific cell populations from fixed tissue sections, by using colorimetric stains, such as immunohistochemistry (IHC), in place of active intervention by a human operator.[10] In xMD, the stained tissue section is brought into close contact with a clear ethylene vinyl acetate (EVA) film and uniformly illuminated with a laser or broad-spectrum light. The energy from the light source is absorbed by the dark stain, causing local melting of the EVA film. When the EVA film is removed, the stained tissue is captured on the film while the unstained tissue is left behind on the glass slide. Initial biological studies with xMD identified unique DNA promoter methylation changes in the tumor microenvironment.[11,12]

Received: March 7, 2013
Accepted: June 25, 2013
Published: June 25, 2013

We recently refined xMD technology by employing a brief pulse of a broad spectrum light source rather than a scanning laser system.[10,12,13] Use of a light flash allows an entire slide to be microdissected effectively and efficiently in milliseconds. Since the resolution of an xMD dissection is determined by the localization of colorimetric stain rather than the focal spot size of a laser beam, subcellular targets such as nuclei can be selectively analyzed with this technique.

In the present manuscript, we describe the proteomic analyses of xMD-procured nuclei from formalin-fixed, paraffin-embedded (FFPE) rat brain tissue, using a new flashcube (flashcube-xMD) system in tandem with a precipitation method that combines biomolecules from multiple films with efficient proteolytic digestion to yield high protein concentration. Enrichment of flashcube-xMD microdissected nuclei is demonstrated using both shotgun and targeted mass spectrometry proteomic analyses and via microscopic visualization.

METHODS

See the Supplementary Methods in the Supporting Information for tissue sectioning, chemicals, and IHC protocols.

Custom Flashcube. A flashcube was built with a xenon flashtube (AQL-1210, Amglo, Bensenville IL) and an elliptical reflector (54-085, Edmund Optics, Barrington NJ) to provide uniform illumination across a 1 in. diameter circle. A Schott GG-400 filter (Edmund Optics, Barrington NJ) prevented UV light from reaching the sample. Flash duration was 150 μs, with a total pulse energy density of approximately 1 J/cm^2 at the sample plane, distributed across the visible spectrum.

Vacuum Chamber. A clamshell-style chamber was designed in Solidworks (Dassault Systémes, Concord MA) and fabricated using a fused deposition modeling 3D printer (Stratasys, Eden Prairie MN). The chamber is connected to a vacuum pump, and a sandwich made of the slide with tissue, capture film, and a large flexible textured film is placed in the chamber. Vacuum transmission across the slide enables close physical contact between the tissue section and the capture film.

Thin EVA Capture Films. Films were made by spincoating thin layers of ethylene vinyl acetate (EVA) from solution onto substrate films of 12.5 μm thick polyethylene terephthalate (PET) (McMaster Carr, Elmhurst IL) using a laboratory spin coater (model WS650-8, Laurell Technologies, North Wales, PA) with a porous vacuum chuck. Films were spun at 1000 rpm from either a 7 wt %/vol solution of EVA-organic acid terpolymer (Elvax 4310, DuPont, Wilmington DE) or a 5 wt %/volume solution of Elvax 410 (DuPont) in toluene. Films had an approximate 600 nm thickness and a <2 nm root-mean-square roughness, as measured by atomic force microscopy of EVA films spun concurrently on glass slides.

Flashcube-xMD. xMD was performed on FFPE rat brain (Pelfreeze biological, Rogers AR) with the flashcube, vacuum holder, and spincoated capture films. For tissue captured using the 4310 films, a piece of heat resistant film (filter no. 398, Rosco Laboratories, Inc., Stamford CT) placed between the flashcube and tissue reduced light transmission and pulse energy to 40%, helping to reduce nonspecific capture. For capture using the 410 films, the heat resistant film used (filter no. 298, Lee Filters, Andover England) reduced light transmission and pulse energy to 70%. Nuclei were microdissected with a vacuum pressure of 350 mm Hg and two pulses of light.

Vacuum Controls. To assess the amount of nonspecific pickup on the EVA films from the effect of the vacuum alone, some samples were treated exactly as the xMD samples except no light pulse from the flashcube was applied.

For xMD with the Arcturus XT (Applied Biosystems, Foster City, CA), a custom-built vacuum chamber was used in place of the standard stage. xMD was performed using the 4310 EVA spincoated films with the IR laser parameters set to 30 μm spot size, 50 ms duration, and 50−100 mW power.

Methanol−Chloroform Precipitation of xMD Tissue. One film with microdissected tissue was put in a 1.5 mL microcentrifuge tube with 200 μL of chloroform and vortexed, dissolving the EVA. The PET backing was removed, the second film with tissue was added and the process repeated. For each sample that was proteolytically digested for mass spectrometry analysis, 2−3 410 films were combined; for the sample analyzed for protein concentration using a BCA assay (see the Supplementary Methods in the Supporting Information), five 4310 films were combined.

A volume of 600 μL of methanol was added to the chloroform/EVA/protein mixture followed by 450 μL of H_2O, vortexing and centrifugation (2 min, 16k × g). Liquid was removed from both the top and the bottom of the tube while preserving the interface. Chloroform was added twice more, each time centrifuging and removing the bottom layer to remove as much EVA as possible. A volume of 450 μL of methanol was added with vortexing and centrifugation (2 min, 16k × g).[14] The supernatant was removed, and the protein pellet was air-dried

Whole Tissue Controls. A clean razorblade was used to scrape the tissue off the glass slide and into 200 μL of chloroform. The sample was precipitated as described above.

Tryptic Digestion. Precipitated protein samples were resuspended in 50% trifluoroethanol (TFE) in 50 mM ammonium bicarbonate (AmBic) (water bath sonication, 45 min). TFE was diluted to 10% with AmBic, and samples were reduced (dithiothreitol, 10 mM, 60 °C, 20 min) and alkylated (iodoacetamide, 25 mM, in the dark, 20 min). Samples were digested with 100 ng of sequencing grade trypsin (Promega, Madison WI) overnight at 37 °C.

After digestion, the sample was adjusted to 5% formic acid, centrifuged to pellet insoluble material (10 min, 16k × g), the supernatant was concentrated to dryness in vacuo (SpeedVac, Thermo Scientific, San Jose, CA) and resuspended in 0.1% formic acid in H_2O. Samples were aliquoted into two tubes and stored at −80 °C until analysis.

Analysis with LTQ-Velos. Resuspended peptides were chromatographed directly on a column, without trap cleanup. The bound peptides were separated at 500 nL/min generating 80−120 bar pressure, using an AQ C18 reverse phase media (3 μm particle size and 200 μm pore) packed in a pulled tip, nanochromatography column (0.100 mm i.d. × 150 mm length) from Precision Capillary Columns, San Clemente, CA. The chromatography was performed in-line with an LTQ-Velos Orbitrap mass spectrometer (ThermoFisher Scientific, West Palm Beach, FL), and the mobile phase consisted of a linear gradient prepared from solvent A (0.1% formic acid in water) and solvent B (0.1% formic acid, 2% water, and 97.9% acetonitrile) at room temperature. Nano LC−MS (LC−MS/MS) was performed with a ProXeon Easy-nLC II multidimensional liquid chromatograph and temperature controlled Ion Max Nanospray source (ThermoFisher Scientific) in-line with the LTQ-Velos Orbitrap mass spectrometer. Computer

controlled data dependent automated switching to MS/MS by Xcalibur 2.1 software was used for data acquisition and provided the peptide sequence information.

Data Analysis. Tandem mass spectra were extracted, charge state deconvoluted, and deisotoped by extract_msn from Xcalibur version 2.0. Samples were analyzed using Mascot (Matrix Science, London, U.K.; version 2.4.0. The SwissProt database (mammalian subset, database downloaded May 29, 2013 [66 262 entries]) was searched assuming tryptic digestion. Searches had fragment ion mass tolerance set at 0.80 Da, parent ion tolerance of 20 ppm, and a fixed modification of alkylated cysteine. Deamidation of asparagine and glutamine, methionine oxidation, and acetylation of the N-terminus were specified in Mascot as variable modifications. Searches for methylation and dimethylation used the rodentia subset of the SwissProt database with a parent ion tolerance of 10 ppm and no other variable modifications specified except for methylation and dimethylation of arginine and lysine

Criteria for Protein Identification. Scaffold (version Scaffold_4.0.3, Proteome Software Inc., Portland, OR) was used to validate peptide and protein identifications. Peptide identifications were ≥95.0% probability.[15] Protein identifications were accepted at ≥99.0% probability with ≥2 identified peptides and were grouped to satisfy the principles of parsimony.[16] Known contaminants (trypsin, keratins, bovine serum albumin, and bovine casein) were not included in the final analysis, though are listed in supplementary Tables 1 and 2 in the Supprting Information.

Localization information for identified proteins was downloaded from the UniProt Web site (www.uniprot.org)[17] and binned into the following categories: cell membrane, cytoplasm, cytoskeleton, ER, ER-translocates, Golgi, Golgi-translocates, membrane, mitochondrion, mitochondrion-translocates, nuclear, nuclear-translocates, perinuclear, ribosome, secreted.

Multiple Reaction Monitoring (MRM). MRM analyses were performed on an Agilent 6490 QqQ with ion-funnel technology and with a chip-cube source attached to a 1260 HPLC and autosampler stack (Agilent Technologies, Santa Clara, CA). Peptides were loaded onto a large capacity C18 chip and separated with a 10-min gradient from 3% to 90% acetonitrile. Crude synthetic peptides with isotopically labeled arginines and lysines were purchased (Thermo Fisher, San Jose, CA) and used for collision energy optimization and elution time determination. Isotopically labeled peptides were spiked into the mixture at a concentration of 50 fmol/μL. Three transitions from both the heavy and light peptides were monitored. Monitored peptides are listed in supplementary Table 3 in the Supporting Information.

Analysis of MRM Samples. All MRM files were imported into Skyline (v1.3, University of Washington) and manually examined to determine the peak presence.[18] For each peptide, the ratio of native to synthetic was recorded. To account for any differences in total amount of protein loaded, each peptide ratio was normalized to the sum of all peptide ratios for each analysis. The resulting value was used to determine fold-change from xMD to whole tissue samples. For graphing purposes, all values were normalized to the average whole-tissue value.

Statistical Analysis. Graphpad Prism 6 was used for statistical analysis. The Student's *t* test using the Holm-Sidak method for multiple comparison corrections was used for analysis.

Scanning Electron Microscopy. 4310 capture films with dissected tissue were mounted with carbon tape and coated with a thin gold layer before imaging with the upper secondary electron detector of an Hitachi S-4800 SEM (Dallas, TX) at 5 kV.

RESULTS

Initial studies demonstrated the ability of the flashcube-xMD to isolate epithelial cells for proteomic analysis, similar to that of traditional LCM methods (see the supplementary text and Figure S1 in the Supporting Information). These initial studies also showed that proteomic analysis of FFPE tissue was equivalent to frozen tissue (see supplementary text and Figure S2 in the Supporting Information).

For nuclear microdissections, commercially available FFPE rat brain was immunostained for Histone H1.0, a general nuclear marker (Figure 1A). The custom-built flashcube for

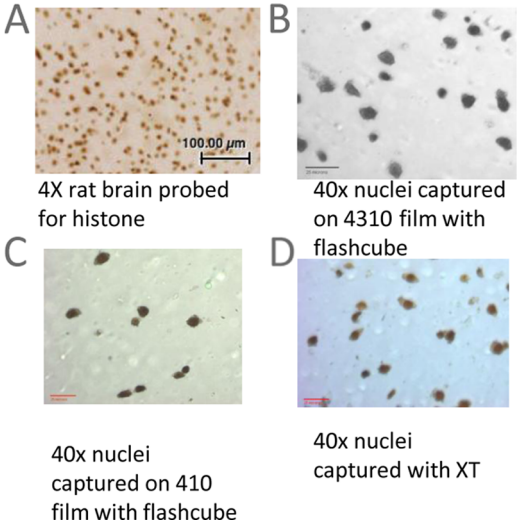

Figure 1. Images of nuclei microdissected from FFPE rat tissue probed for Histone H1.0: (A) coverslipped rat brain prior to microdissection, (B) nuclei microdissected onto 4310 EVA film using flashcube-xMD (bar is equal to 25 μm), (C) nuclei microdissected onto 410 EVA film using flashcube-xMD (bar is equal to 25 μm), and (D) nuclei microdissected onto 4310 EVA film using an Arcturus XT LCM instrument (bar is equal to 25 μm).

flashcube-xMD successfully captured the nuclei, as determined by light microscopy (Figure 1B,C). Similar results were obtained, albeit with much longer dissection times, using a modified Arcturus XT LCM instrument (Figure 1D), demonstrating that xMD subcellular microdissection can be successfully performed by several devices.[13] Additionally, two types of films were examined, the 4310 and 410 films. Visual inspection suggested that the specific capture for either the 4310 (Figure 1B) or 410 (Figure 1C) films was very similar, though it was observed that the 410 films exhibited less nonspecific pickup than the 4310 films (supplementary text and Figure S4 in the Supporting Information).

Scanning electron microscopy (SEM) was used to image the captured nuclei on the 4310 EVA film (low magnification overview, Figure 2A). An example SEM image shows two captured nuclei next to each other, with little to no connecting tissue observed between the nuclei, indicating the technique can specifically dissect only stained organelles without capturing adjacent unstained tissue (Figure 2B). The specificity of xMD dissections is consistent with previously reported studies.[10] A single xMD captured nucleus measures approx-

dx.doi.org/10.1021/ac400691k | *Anal. Chem.* 2013, 85, 7139−7145

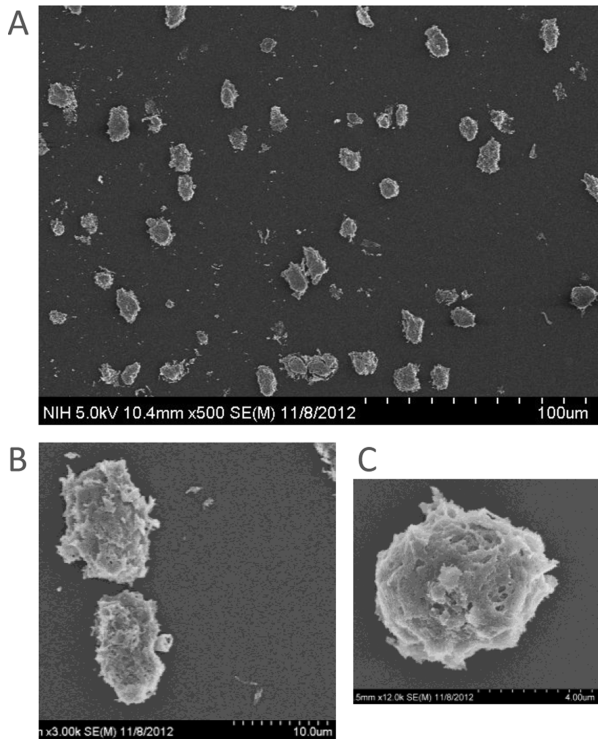

Figure 2. Scanning electron microscopy (SEM) of nuclei microdissected from FFPE rat brain using 4310 EVA films and the flashcube: (A) low-magnification SEM showing many captured nuclear structures, (B) two adjacent nuclei, and (C) a single nucleus.

imately 6 μM in diameter, an expected size for a mammalian nucleus (Figure 2C).[19]

Initial attemps at on-film digestion of captured nuclei proved to be inefficient at removing protein from the film and yielded subpar LC–MS/MS analysis (data not shown). Therefore, a method was devised to combine multiple xMD films and remove captured tissue from the films prior to proteolytic digestion, thereby improving total protein yield (see Figure 3). As the EVA is soluble in chloroform, tissue from multiple films can be easily combined with a modified methanol–chloroform protein precipitation method.[14] A BCA assay of the resuspended precipitate demonstrated that there was roughly 400 ng of protein per film (see Supplementary Methods in the Supporting Information).

For LC–MS/MS analysis, nonmicrodissected rat brain tissue sections were compared to flashcube-xMD nuclei of rat brain. A total of four flashcube-xMD samples (approximately 400–700 ng of protein per sample) and four whole tissue samples (approximately 700 ng of protein for each sample) were analyzed by LC–MS/MS on an LTQ-Velos. The number of identified proteins was equivalent for the flashcube-xMD and whole tissue samples (762 ± 52 and 749 ± 22, respectively). Please see supplementary Tables 1 and 2 in the Supporting Information for additional data.

The subcellular location for each identified protein from either the whole tissue or flashcube-xMD LC–MS/MS analyses was obtained from the UniProt Web site (listed in the supplementary text, Figure S4, and supplementary Table 1 in the Supporting Information).[17] On average, for the flashcube-xMD samples, 25% of recovered proteins localized to the nucleus or perinuclear region (Figure 4A), significantly higher

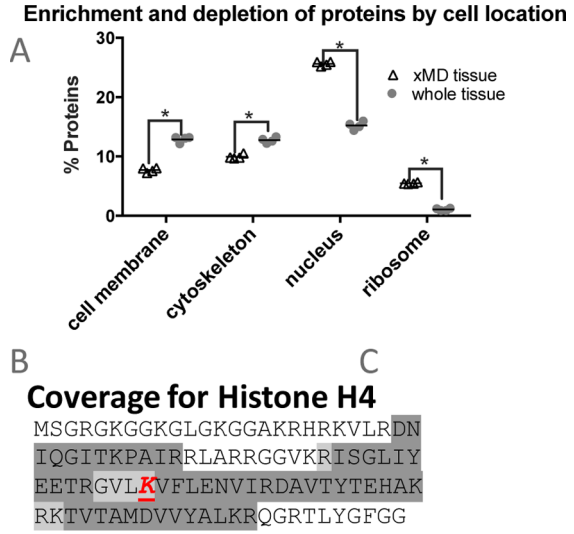

Figure 4. Percentage of identified proteins localized to nucleus is increased in xMD samples compared to whole tissue samples. (A) Scatter plot showing the average number of recovered proteins for the xMD and whole tissue samples that had the following UniProt localization categories: cell membrane, cytoskeleton, nucleus, ribosome. $N = 4$, $^*p < 0.001$, Student's two-tailed t test for nonpaired samples, adjusted for multiple comparisons. (B) Sequence coverage for the Histone H4 protein, a nuclear protein identified in both the xMD and whole tissue samples. Sequence highlighted in dark gray was identified in both samples, and light gray was identified in only xMD samples. Bolded lysine was identified as methylated only in the xMD samples.

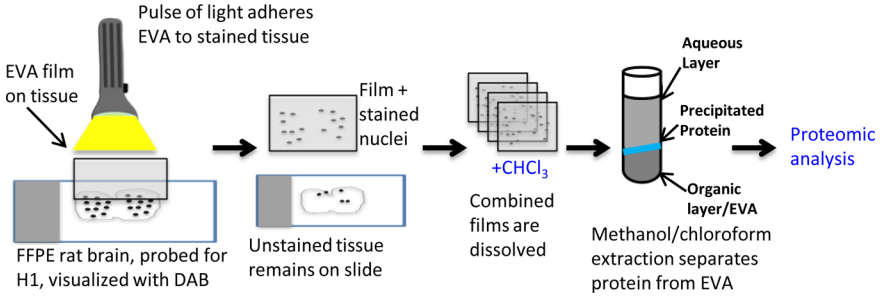

Figure 3. Preparation of microdissected nuclei for downstream proteomic analysis. Each rat brain section was covered with a thin EVA film on a clear PET backing. The whole tissue was exposed to light at once. Following flashcube-xMD, multiple EVA films were combined with chloroform. The chloroform dissolved the EVA and released the captured nuclei. Protein extraction was achieved using a modified methanol/chloroform protein precipitation. The sample was digested with trypsin and analyzed using LC–MS/MS or MRM methods.

dx.doi.org/10.1021/ac400691k | *Anal. Chem.* 2013, 85, 7139–7145

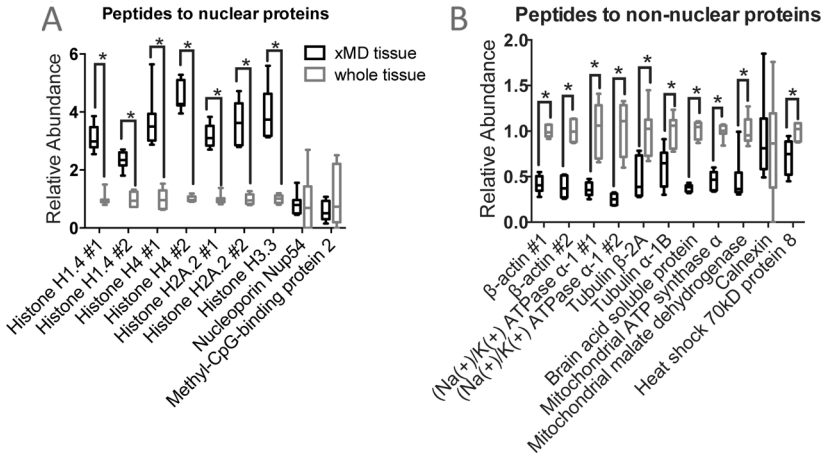

Figure 5. MRM analysis of flashcube-xMD and whole tissue samples. Eight flashcube-xMD samples were analyzed and seven whole tissue samples were analyzed. Statistical significance was assessed using a Student's *t* test with the Holm-Sidak method to correct for multiple comparisons, $*p < 0.01$. (A) Box plots of relative abundance in all monitored peptides belonging to nuclear localized proteins. For some proteins, multiple peptides were monitored-those different peptides are marked as #1 or #2 in the *X*-axis titles. (B) Box plots of relative abundance in all monitored peptides belonging to non-nuclear localized proteins. For some proteins, multiple peptides were monitored, those different peptides are marked as #1 or #2 in the *X*-axis titles.

($p < 0.001$) than the whole tissue samples, which on average had 15% of recovered proteins that localized to the nucleus (Figure 4A). This significant increase in nuclear proteins was accompanied by an increase in ribosomal proteins and a decrease in proteins that localize to the cell membrane and cytoskeleton. While this increase in nuclear protein recovery seems modest, it still afforded identifications of proteins not seen in the whole tissue samples and increased sequence coverage of identified nuclear proteins. A total of 248 proteins were identified solely in the flashcube-xMD samples and not the whole tissue samples, including Histone H1.0, the antibody target (supplementary Table 1 and 2 in the Supporting Information). Histone H4 was identified with 12 unique peptides in the flashcube-xMD samples, including a peptide identifying a methylated lysine (K60), whereas in the whole tissue samples it was identified with only 7 unique peptides, none of which identified any biological modifications (Figure 4B).

To further assess the nuclear enrichment of the flashcube-xMD samples, multiple reaction monitoring (MRM) was performed (Figures 5 and 6), targeting peptides that had been observed in preliminary shotgun proteomic analyses from proteins with well characterized localization information. A full list of peptides that were successfully targeted is listed in supplementary Table 3 in the Supporting Information.

Eight flashcube-xMD samples and seven whole tissue samples were analyzed using MRM. A total of 21 peptides from 15 different proteins with known cellular localizations were quantified. Peptides corresponding to four histones all show enrichment in the flashcube-xMD samples, compared to the whole tissue samples (Figure 5A). Interestingly, peptides belonging to two other nuclear proteins, Nuclear pore 54 (NUP54) and Methyl-CpG binding protein (MeCP2) did not show enrichment in the xMD samples.

Peptide abundances from proteins localized to the cytoplasm, cytoskeleton, and mitochondria are increased in the whole tissue samples and show depletion in the flashcube-xMD samples (Figure 5B). The protein marker for the endoplasmic reticulum, calnexin, shows no significant change in abundance between the flashcube-xMD and whole tissue samples.

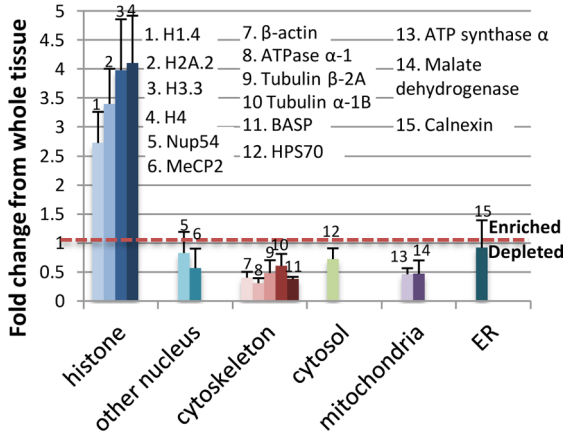

Figure 6. Protein enrichment and depletion demonstrated by MRM analysis. Peptides monitored by MRM were mapped back to proteins (if multiple peptides were from the same protein, their relative abundances were averaged together). The ratio of abundance from flashcube-xMD to abundance from whole tissue samples was taken, and proteins were binned to their subcellular localization. A relative abundance greater than 1 means the protein is enriched in flashcube-xMD samples relative to whole tissue samples.

Examining the proteins that show enrichment and depletion in the flashcube-xMD samples (Figure 6), there is clear enrichment for histones, the protein complex specifically targeted by the antibody for microdissection and depletion of non-nuclear proteins.

DISCUSSION AND CONCLUSION

Our data demonstrate that the use of the flashcube-xMD technology enriches for nuclei in FFPE tissue and that IHC stained, flashcube-xMD-acquired samples are amenable to peptide identification with mass spectrometry. Our focus on FFPE tissue in this report was to adapt the flashcube-xMD technology to the most commonly used method of tissue fixation in pathology, thus optimizing the number of possible downstream clinical applications. The flashcube-xMD technique facilitated the high-throughput capture of nuclei. The

dx.doi.org/10.1021/ac400691k | *Anal. Chem.* 2013, 85, 7139−7145

collection of up to 2 μg of nuclei takes less than a half hour with this technique; using LCM, procurement of the same amounts of tissue can take an entire day.

Importantly, peptides matching to antibodies were not identified, demonstrating that IHC staining does not result in an overwhelming signal from antibody chains.[20] Additionally, peptides matching to the antigen, Histone H1.0, were identified solely in the flashcube-xMD samples, demonstrating enrichment of the target.

Previously published methods for nuclear enrichment rely on the use of fresh or frozen tissue that had not been subjected to formalin fixation. These proteomic analyses of nuclei isolated from fresh or flash-frozen cell lines or tissue report a wide range of nuclear enrichment, from ∼40% (roughly 2.5-fold enrichment)[21] to 60%[22] to 84%[23] of recovered proteins as localized at least part-time to the nucleus. In two of these publications, it is unclear what the percentage of proteins from the starting material (prior to nuclear enrichment) localized to the nucleus, and thus unclear exactly how much enrichment for nuclear proteins is obtained.

There are many reports in the literature of FFPE whole tissue proteomic analysis,[24,6,25−28] and initial reports suggest that these samples are *not* inherently biased against specific subcellular organelles.[29] While the flashcube-xMD microdissected samples showed a significant enrichment for nuclear proteins, only 25% of the identified proteins are characterized as nuclear, a noticeably lower number than reports using nonformalin fixed tissue. However, the technical inability to fractionate FFPE tissue using traditional organellar enrichment methods demonstrates the potential importance of this technique to the field.

It should also be noted that protein localization information can be an imprecise measure of enrichment as most proteins are not well characterized with regard to compartmentalization. The MRM data shows compelling evidence of nuclear enrichment (Figures 5 and 6), with significantly lower abundance for non-nuclear proteins relative to histones in the xMD samples as compared to the whole tissue samples. The two other nuclear proteins that were targeted, MeCP2 and NUP54, did not show significant enrichment in the xMD samples. It is unclear why these proteins do not show enrichment; they might be predominantly present in nuclei that were unstained (and thus not captured using flashcube-xMD), or reside in parts of the nucleus that did not get reliably captured with the flashcube-xMD. The LTQ-Velos proteomic profile data (supplementary Table 1 in the Supporting Information) identified many proteins associated with the nuclear envelope (similar to NUP54) or that are DNA-binding proteins (similar to MeCP2) that were enriched or identified exclusively in the flashcube-xMD samples, suggesting that a wide variety of nuclear-localized proteins were captured in the flashcube-xMD samples.

Continued improvements in the flashcube-xMD method should improve the isolation and enrichment of nuclei and allow for further proteomic profiling. However, the xMD method presented here can readily be used for experiments in FFPE tissue where enrichment for specific immunoreactive targets is desired, for example, the characterization of nuclei from only a particular subset of cells in a tissue as we discuss below.

Despite the generally positive results in the current study, there are several technical caveats that one should consider when using xMD for retrieval of nuclei (or other cellular organelles) in the future. First, because FFPE histological sections are thin (typically only 5 μm), the xMD process is almost certainly extracting some transected partial nuclei. These partial nuclei contain histone complexes (and thus are successfully stained during IHC), but some might be lacking other parts of the nucleus, such as the nuclear envelope or the nucleolus. Conversely, if only a partial nucleus is stained, there might be non-nuclear tissue directly above or below the stained nucleus in the *z*-plane, which is inherent in tissue analysis. The non-nuclear tissue would be captured along with the nuclear tissue, and this could lead to minor contamination in the sample. It is also possible that some non-nuclear tissue adjacent to captured nuclei can get captured as well, resulting in additional contamination. It is noted that in the profile data, a significant increase in ribosomal proteins was observed (Figure 4), and in the MRM data (Figures 5 and 6) Calnexin, a resident ER protein, was not depleted in the nuclear sample, suggesting that some endoplasmic reticulum may get captured with the nuclei.

For the work here, we collected a relatively large number of randomly positioned nuclei and thus suspect any sectioning effect was "normalized" and had little effect on the data. While it is possible that the microdissection of partial nuclei could affect our results (and might be one reason why NUP54 and MeCP2 did not show enrichment in the xMD samples), this is beyond the scope of this initial report.

Flashcube-xMD could be used to retrieve only organelles that stain positive for a known biomarker of disease. For example, nuclei that are only positive for the estrogen or progesterone receptors (ER or PR) could be microdissected from breast cancer tissue or TTF-1 positive nuclei could be microdissected from lung cancer specimens. This would allow researchers to specifically profile only the organelles from a select populations of cancer cells to better identify proteins that are potentially involved in tumor progression or heterogeneity. The ability to selectively capture immuno-stained nuclei from fixed tissue in a high-throughput manner for downstream proteomic analysis has the potential to improve our understanding of disease-state proteomes.

■ ASSOCIATED CONTENT

Supporting Information

Supporting text and supporting Excel tables. This material is available free of charge via the Internet at http://pubs.acs.org.

■ AUTHOR INFORMATION

Corresponding Author

*E-mail: buckm@mail.nih.gov.

Notes

The authors declare no competing financial interest.

■ ACKNOWLEDGMENTS

This work was supported in part by the intramural program at the NIH (Grants ZIA MH002919 and 1ZIABC010729), including the Center for Cancer Research, NCI, NIBIB, and an NIH Directors award. Special thanks goes to the NIAID Research Technologies Branch for sample analysis and bioinformatics assistance. Thanks to Kris Ylaya and Qiang Du, M.D. for tissue sectioning and to Jeff Hanson for assistance with the Arcturus XT instrument. We benefitted from helpful technical discussions and assistance from NIH scientists J. Lippincott-Schwartz, C. Ott, D. Sackett, D. Johann, B. Martin, J.

Kowalak, A. J. Makusky, M. Gucek, and A. Aponte. The loan from Agilent of a 6490 triple quadrupole mass spectrometer with chipcube and 1260 HPLC and autosampler stack contributed to the successful MRM analyses and is gratefully acknowledged.

REFERENCES

(1) Emmert-Buck, M. R.; Bonner, R. F.; Smith, P. D.; Chuaqui, R. F.; Zhuang, Z.; Goldstein, S. R.; Weiss, R. A.; Liotta, L. A. *Science* **1996**, *274*, 998−1001.
(2) Yan, W.; Shih, J. H.; Rodriguez-Canales, J.; Tangrea, M. A.; Ylaya, K.; Hipp, J.; Player, A.; Hu, N.; Goldstein, A. M.; Taylor, P. R.; Emmert-Buck, M. R.; Erickson, H. S. *BMC Res. Notes* **2012**, *5*, 73.
(3) Ly, L.; Barnett, M. H.; Zheng, Y. Z.; Gulati, T.; Prineas, J. W.; Crossett, B. *J. Proteome Res.* **2011**, *10*, 4855−4868.
(4) Arentz, G.; Chataway, T.; Price, T. J.; Izwan, Z.; Hardi, G.; Cummins, A. G.; Hardingham, J. E. *Clin. Proteomics* **2011**, *8*, 16.
(5) Liu, N. Q.; Braakman, R. B.; Stingl, C.; Luider, T. M.; Martens, J. W.; Foekens, J. A.; Umar, A. *J. Mammary Gland Biol. Neoplasia* **2012**, *17*, 155−164.
(6) Bateman, N. W.; Sun, M.; Bhargava, R.; Hood, B. L.; Darfler, M. M.; Kovatich, A. J.; Hooke, J. A.; Krizman, D. B.; Conrads, T. P. *J. Proteome Res.* **2011**, *10*, 1323−1332.
(7) Besson, D.; Pavageau, A. H.; Valo, I.; Bourreau, A.; Bélanger, A.; Eymerit-Morin, C.; Moulière, A.; Chassevent, A.; Boisdron-Celle, M.; Morel, A.; Solassol, J.; Campone, M.; Gamelin, E.; Barré, B.; Coqueret, O.; Guette, C. *Mol. Cell. Proteomics* **2011**, *10*, M111.009712.
(8) Lu, Q.; Murugesan, N.; Macdonald, J. A.; Wu, S. L.; Pachter, J. S.; Hancock, W. S. *Electrophoresis* **2008**, *29*, 2689−2695.
(9) Goldstein, S. R.; McQueen, P. G.; Bonner, R. F. *Appl. Opt.* **1998**, *37*, 7378−7391.
(10) Tangrea, M. A.; Chuaqui, R. F.; Gillespie, J. W.; Ahram, M.; Gannot, G.; Wallis, B. S.; Best, C. J.; Linehan, W. M.; Liotta, L. A.; Pohida, T. J.; Bonner, R. F.; Emmert-Buck, M. R. *Diagn. Mol. Pathol.* **2004**, *13*, 207−212.
(11) Grover, A. C.; Tangrea, M. A.; Woodson, K. G.; Wallis, B. S.; Hanson, J. C.; Chuaqui, R. F.; Gillespie, J. W.; Erickson, H. S.; Bonner, R. F.; Pohida, T. J.; Emmert-Buck, M. R.; Libutti, S. K. *J. Transl. Med.* **2006**, *4*, 13.
(12) Hanson, J. A.; Gillespie, J. W.; Grover, A.; Tangrea, M. A.; Chuaqui, R. F.; Emmert-Buck, M. R.; Tangrea, J. A.; Libutti, S. K.; Linehan, W. M.; Woodson, K. G. *J. Natl. Cancer Instit.* **2006**, *98*, 255−261.
(13) Hanson, J. C.; Tangrea, M. A.; Kim, S.; Armani, M. D.; Pohida, T. J.; Bonner, R. F.; Rodriguez-Canales, J.; Emmert-Buck, M. R. *Nat. Protoc.* **2011**, *6*, 457−467.
(14) Wessel, D.; Flügge, U. I. *Anal. Biochem.* **1984**, *138*, 141−143.
(15) Keller, A.; Nesvizhskii, A. I.; Kolker, E.; Aebersold, R. *Anal. Chem.* **2002**, *74*, 5383−5392.
(16) Nesvizhskii, A. I.; Keller, A.; Kolker, E.; Aebersold, R. *Anal. Chem.* **2003**, *75*, 4646−4658.
(17) Consortium, U. *Nucleic Acids Res.* **2012**, *40*, D71−D75.
(18) MacLean, B.; Tomazela, D. M.; Shulman, N.; Chambers, M.; Finney, G. L.; Frewen, B.; Kern, R.; Tabb, D. L.; Liebler, D. C.; MacCoss, M. J. *Bioinformatics* **2010**, *26*, 966−968.
(19) Hockmuth, C.; Fujioka, A.; Terai, K.; Itoh, R. E.; Aoki, K.; Nakamura, T.; Kuroda, S.; Nishida, E.; Matsuda, M. *J. Biol. Chem.* **2006**, *281*, 8917−8926.
(20) Tangrea, M. A.; Mukherjee, S.; Gao, B.; Markey, S. P.; Du, Q.; Armani, M.; Kreitman, M. S.; Rosenberg, A. M.; Wallis, B. S.; Eberle, F. C.; Duncan, F. C.; Hanson, J. C.; Chuaqui, R. F.; Rodriguez-Canales, J.; Emmert-Buck, M. R. *J. Histochem. Cytochem.* **2011**, *59*, 591−600.
(21) Liao, L.; McClatchy, D. B.; Park, S. K.; Xu, T.; Lu, B.; Yates, J. R., 3rd. *J. Proteome Res.* **2008**, *7*, 4743−4755.
(22) Desrivieres, S.; Kuhn, K.; Muller, J.; Glaser, M.; Laria, N. C.; Korder, J.; Sonnentag, M.; Neumann, T.; Schwarz, J.; Schafer, J.; Hamon, C.; Groner, B.; Prinz, T. *Proteomics* **2007**, *7*, 2019−2037.
(23) Bennetzen, M. V.; Larsen, D. H.; Bunkenborg, J.; Bartek, J.; Lukas, J.; Andersen, J. S. *Mol. Cell. Proteomics* **2010**, *9*, 1314−1323.
(24) Alkhas, A.; Hood, B. L.; Oliver, K.; Teng, P. N.; Oliver, J.; Mitchell, D.; Hamilton, C. A.; Maxwell, G. L.; Conrads, T. P. *J. Proteome Res.* **2011**, *10*, 5264−5271.
(25) Fountzilas, G.; Dafni, U.; Bobos, M.; Batistatou, A.; Kotoula, V.; Trihia, H.; Malamou-Mitsi, V.; Miliaras, S.; Chrisafi, S.; Papadopoulos, S.; Sotiropoulou, M.; Filippidis, T.; Gogas, H.; Koletsa, T.; Bafaloukos, D.; Televantou, D.; Kalogeras, K. T.; Pectasides, D.; Skarlos, D. V.; Koutras, A.; Dimopoulos, M. A. *PLoS One* **2012**, *7*, e37946.
(26) Fowler, C. B.; O'Leary, T. J.; Mason, J. T. *Methods Mol. Biol.* **2011**, *724*, 281−295.
(27) Sprung, R. W.; Martinez, M. A.; Carpenter, K. L.; Ham, A.-J.; Washington, M. K.; Arteaga, C.; Sanders, M.; Liebler, D. C. *J. Proteome Res.* **2012**, *11*, 3498−3505.
(28) Scicchitano, M. S.; Dalmas, D. A.; Boyce, R. W.; Thomas, H. C.; Frazier, K. S. *J. Histochem. Cytochem.* **2009**, *57*, 849−860.
(29) Sprung, R. W., Jr.; Brock, J. W.; Tanksley, J. P.; Li, M.; Washington, M. K.; Slebos, R. J.; Liebler, D. C. *Mol. Cell. Proteomics* **2009**, *8*, 1988−1998.